High-Sensitivity Piezoelectric, Low-Tolerance-Factor Perovskites by Mechanosynthesis

M. Algueró,[†] J. Ricote,[†] T. Hungría,[†,‡] and A. Castro*,[†]

Instituto de Ciencia de Materiales de Madrid, CSIC, Cantoblanco, 28049 Madrid, Spain, and Centre d'Elaboration de Matériaux et d'Etudes Structurales, CNRS, 29 rue Jeanne Marvig, BP 94347, 31055 Toulouse, France

Received June 20, 2007. Revised Manuscript Received July 17, 2007

Ferroelectric low-tolerance-factor perovskites are gathering a lot of attention in the search for novel perovskite solid solutions with a morphotropic phase boundary, which present the highest piezoelectric coefficients known. However, thermodynamic stability is an issue, and powders and ceramics of a number of compositions in very promising systems cannot be synthesized and processed but by high-pressure techniques. This is the case of $Pb(Zn_{1/3}Nb_{2/3})O_3-PbTiO_3$ with piezoelectric coefficients as high as 2500 pC N^{-1} and of the $BiMO_3-PbTiO_3$ (M for metal) systems with a high Curie temperature, which are anticipated to enable high sensitivity at temperatures above 300 °C. We report here mechanochemical activation experiments on $0.92Pb(Zn_{1/3}Nb_{2/3})O_3-0.08PbTiO_3$ that strongly suggest that mechanosynthesis is a good alternative for preparing high-sensitivity piezoelectric, low-tolerance perovskite materials. This is demonstrated by processing ceramics of the $Pb(Zn_{1/3}Nb_{2/3})O_3-Pb(Fe_{1/2}Nb_{1/2})O_3-PbTiO_3$ and $BiScO_3-PbTiO_3$ systems from mechanosynthesized powders. Stabilization mechanisms are discussed, and associated effects are established.

Introduction

Piezoelectric, ferroelectric $Pb(Zr_xTi_{1-x})O_3$ (PZT) ceramics with a perovskite structure are the basis of a large number of electromechanical transduction technologies, such as sensors and actuators, ultrasound generation and sensing, and underwater acoustics.[1] The highest piezoelectric coefficients are provided by compositions around the morphotropic phase boundary (MPB) between the rhombohedral and tetragonal phases at $x \approx 0.53$[2,3] and are associated with the existence of a monoclinic phase[4,5] and a mechanism of polarization rotation among the phases.[6,7] This is the same mechanism responsible for the ultrahigh piezoelectricity of $Pb(Zn_{1/3}Nb_{2/3})O_3-PbTiO_3$ (PZN−PT) and $Pb(Mg_{1/3}Nb_{2/3})O_3-PbTiO_3$ (PMN−PT) single crystals with composition close to their MPBs.[8,9] These crystals present effective d_{33} coefficients as high as 2500 pC N^{-1} along the ⟨001⟩ direction, which have to be compared with ∼600 pC N^{-1} for commercial soft PZT ceramics, and have thus the potential to enable a new generation of highly improved sensitivity piezoelectric devices.[10] However, crystals are grown in PbO flux under stringent and time-consuming (several days) temperature profiles,[11] and a lot of effort is being put into the preparation of ceramics with a ⟨001⟩ preferred orientation as an alternative; textured PMN−PT ceramics have already been obtained with piezoelectric coefficients of 1600 pC N^{-1}.[12,13] The enhancement of piezoelectric activity by texturing of perovskite solid solutions with MPB is a general concept that has allowed an environmentally friendly, lead-free piezoelectric ceramic with piezoelectric coefficients comparable to those of PZT to be obtained[14] and is also leading the search for novel high-temperature piezoelectrics[15] in response to the strong demand for high sensitivity above 300 °C.

However, many of these materials are difficult to prepare. This is the case of PZN−PT, for which the processing of ceramics remains a challenge. Attempts to synthesize PZN−PT ceramic powders by solid-state reaction of oxides or from chemical solution derived precursors have failed, and a pyrochlore-type phase always results.[16,17] Unlike PMN−PT, for which pyrochlore phases appear because of the low

[†] CSIC.
[‡] CNRS.

(1) *Piezoelectric Materials in Devices*; Setter, N., Ed.; Lausanne, 2002.
(2) Jaffe, B.; Cook, W. R.; Jaffe, H. *Piezoelectric Ceramics*; Academic Press: London, 1971.
(3) Cao, W.; Cross, L. E. *Phys. Rev. B* **1993**, *47*, 4825.
(4) Noheda, B.; Cox, D. E.; Shirane, G.; Gonzalo, J. A.; Cross, L. E.; Park, S. E. *Appl. Phys. Lett.* **1999**, *74*, 2059.
(5) Noheda, B.; Gonzalo, J. A.; Cross, L. E.; Guo, R.; Park, S. E.; Cox, D. E.; Shirane, G. *Phys. Rev. B* **2000**, *61*, 8687.
(6) Guo, R.; Cross, L. E.; Park, S. E.; Noheda, B.; Cox, D. E.; Shirane, G. *Phys. Rev. Lett.* **2000**, *84*, 5423.
(7) Fu, H. X.; Cohen, R. E. *Nature* **2000**, *403*, 281.
(8) Park, S. E.; Shrout, T. R. *J. Appl. Phys.* **1997**, *82*, 1804.
(9) Noheda, B.; Cox, D. E.; Shirane, G.; Park, S. E.; Cross, L. E.; Zhong, Z. *Phys. Rev. Lett.* **2001**, *86*, 3891.
(10) Service, R. F. *Science* **1997**, *275*, 1878.
(11) Mulvihill, M. L.; Park, S. E.; Risch, G.; Li, Z.; Uchino, K. *Jpn. J. Appl. Phys.* **1996**, *35*, 3984.
(12) Sabolsky, E. M.; James, A. R.; Kwon, S.; Trolier-McKinstry, S.; Messing, G. L. *Appl. Phys. Lett.* **2001**, *78*, 2551.
(13) Kwon, S.; Sabolsky, E. M.; Messing, G. L.; Trolier-McKinstry, S. *J. Am. Ceram. Soc.* **2005**, *88*, 312.
(14) Saito, Y.; Takao, H.; Tani, T.; Nonoyama, T.; Takatori, K.; Homma, T.; Nagaya, T.; Nakamura, N. *Nature* **2004**, *432*, 84.
(15) Eitel, R. E.; Randall, C. A.; Shrout, T. R.; Rehrig, P. W.; Hackenberger, W.; Park, S. E. *Jpn. J. Appl. Phys.* **2001**, *40*, 5999.
(16) Gururaja, T. R.; Safari, A.; Halliyal, A. *Am. Ceram. Soc. Bull.* **1986**, *65*, 1601.
(17) Hayes, J. M.; Gururaja, T. R.; Geoffroy, G. L.; Cross, L. E. *Mater. Lett.* **1987**, *5*, 396.

10.1021/cm071656v CCC: $37.00
Published on Web 09/08/2007

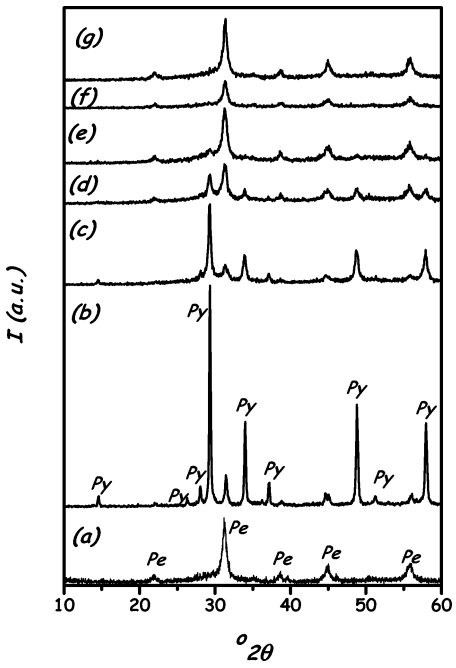

Figure 1. XRD patterns of (a) the nanocrystalline 0.92PZN−0.08PT perovskite powder obtained by mechanochemical activation of the oxides for 70 h and (b) the same powder after heating at 700 °C. Patterns of the pyrochlore powder of (b) after mechanochemical activation for (c) 1 h, (d) 4 h, (e) 8 h, (f) 12 h, and (g) 16 h. Pe = perovskite, and Py = pyrochlore.

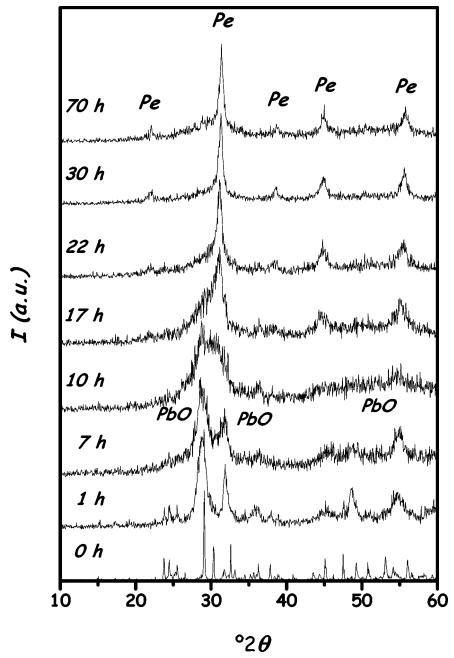

Figure 2. XRD patterns of the 0.82PZN−0.1PFN−0.08PT precursor powder after mechanochemical activation at increasing times. Pe = perovskite.

reactivity of MgO,[18] difficulties with PZN−PT are rather an issue of thermodynamical stability than of kinetics;[19] single crystals decompose into a pyrochlore phase and PbO during heating at temperatures between 600 and 1200 °C.[20] The stability of ABO_3 perovskites has been discussed on the basis of the ionic radii of the cations with Goldschmidt's tolerance factor, *t*;[21] it was concluded that the structure is stable within a *t* range between 0.88 and 1.09. A plot of this factor against the average electronegativity difference between cations and anions for a number of perovskites suggests that the stability increases with both magnitudes and shows that PZN presents both a tolerance factor ($t = 0.986$) and an electronegativity difference among the lowest.[17] Besides in PbO flux, the phase was only obtained by high-pressure synthesis from a mixture of oxides[22] and from the pyrochlore phase that results from the solid-state reaction of the oxides, also by hot isostatic pressing.[23] Significantly lower pressures, 150−200 MPa as compared with 2.5 GPa, were necessary in the latter case.

Thermodynamic stability is also an issue in the perovskite systems under consideration for high-temperature applications. It has been shown that there is an empirical relation between the Curie temperature of the MPB composition in a $PbTiO_3$-based system and the tolerance factor of the rhombohedral end member in solid solution with PT, so the Curie temperature increases as the tolerance factor decreases.[15] Therefore, attention has focused on low-tolerance-factor perovskites, among which $BiMO_3$ (M for metal) ones are being extensively explored. MPBs with a Curie temperature higher than that of PZT have been found for a limited number of systems,[24−26] but the lack of stability has prevented the preparation of other promising MPB materials[15] and of most of the $BiMO_3$-rich compositions of the solid solutions.[27] A lot of effort has concentrated on $(1 - x)BiScO_3-xPbTiO_3$, for which the MPB has been reported at $x \approx 0.64$ ($t = 0.98$) and ceramics have been processed successfully with a piezoelectric coefficient of 450 pC N^{-1}, but for which compositions with $x \leq 0.5$ ($t \leq 0.96$) have only been prepared, like PZN−PT, under high pressure.[28]

Although high-pressure techniques can synthesize these low-tolerance-factor perovskites, they only provide very small amounts of material and, therefore, do not allow systematic studies on the processing of ceramics and on their functional properties. The thorough investigation of these systems and the search for novel solid solutions with a morphotropic phase boundary for developing new high-sensitivity materials require finding alternatives to high-pressure techniques that provide enough material for addressing the processing of ceramics and the full assessment of their functionality.

We show here that mechanochemical activation can play this role. This is a powerful technique for the preparation of

(18) Swartz, S. L.; Shrout, T. R. *Mater. Res. Bull.* **1982**, *17*, 1245.
(19) Halliyal, A.; Kumar, U.; Newham, R. E.; Cross, L. E. *Am. Ceram. Soc. Bull.* **1987**, *66*, 671.
(20) Jang, H. M.; Oh, S. H.; Moon, J. H. *J. Am. Ceram. Soc.* **1992**, *75*, 82.
(21) Goldschmidt, V. M. *Geochemisca Veterlun*; Norske Videnkap: Oslo, 1927.
(22) Matsuo, Y.; Sasaki, H.; Hayakawa, S.; Kanamaru, F.; Kuizumi, M. *J. Am. Ceram. Soc.* **1969**, *52*, 516.
(23) Fujiu, T.; Tanaka, A.; Takenaka, T. *Jpn. J. Appl. Phys.* **1991**, *30* (2B), L298.
(24) Eitel, R. E.; Randall, C. A.; Shrout, T. R.; Park, S. E. *Jpn. J. Appl. Phys.* **2002**, *41*, 2099.
(25) Cheng, J.; Eitel, R.; Li, N.; Cross, L. E. *J. Appl. Phys.* **2003**, *94*, 605.
(26) Randall, C. A.; Eitel, R.; Jones, B.; Shrout, T. R.; Woodward, D. I.; Reaney, I. M. *J. Appl. Phys.* **2004**, *95*, 3633.
(27) Eitel, R. E.; Zhang, S. J.; Shrout, T. R.; Randall, C.; Levin, I. *J. Appl. Phys.* **2004**, *96*, 2828.
(28) Inaguma, Y.; Miyaguchi, A.; Yoshida, M.; Katsumata, T.; Shimojo, Y.; Wang, R.; Sekiya, T. *J. Appl. Phys.* **2004**, *95*, 231.

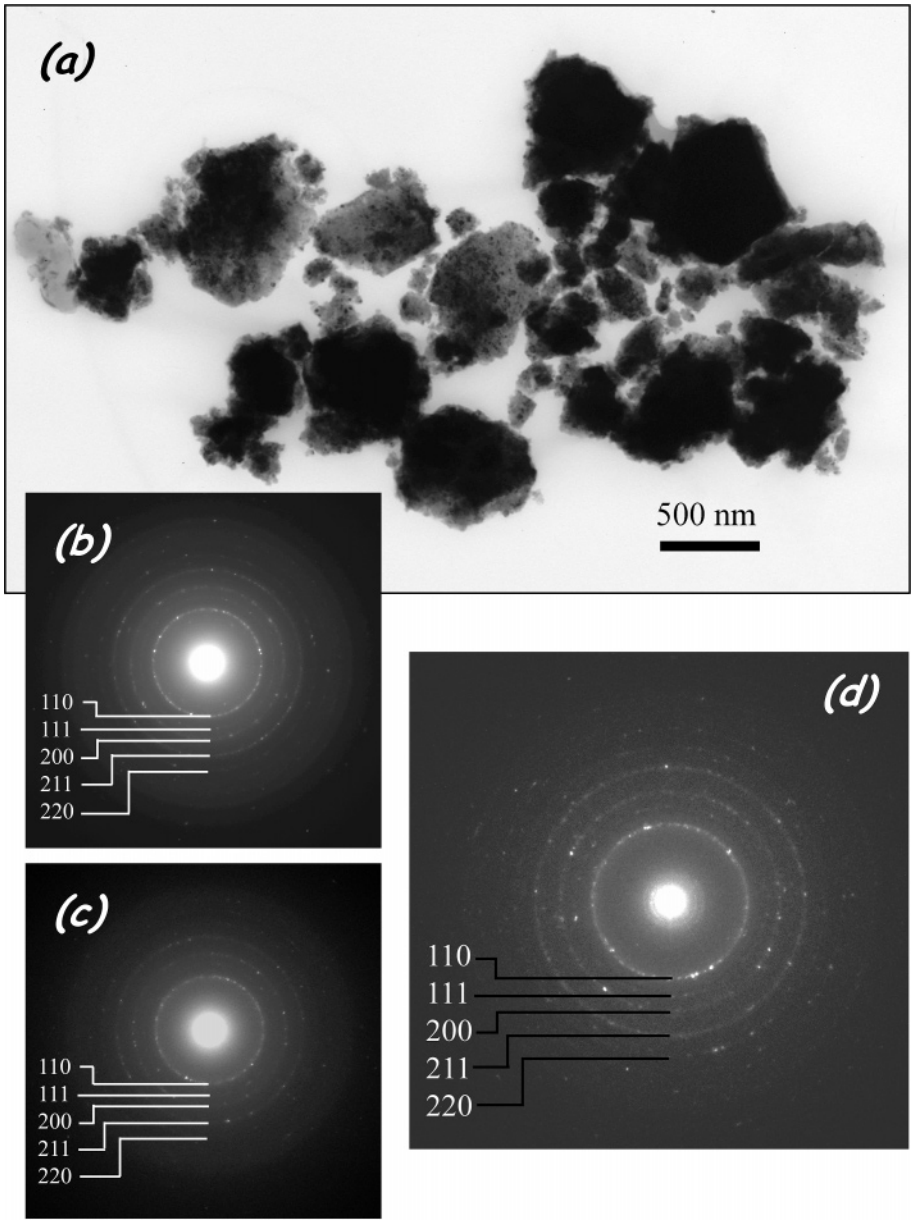

Figure 3. Transmission electron microscopy image of the 0.82PZN−0.1PFN−0.08PT powder obtained by mechanochemical activation for 30 h (a) and selected area electron diffraction of the 0.82PZN−0.1PFN−0.08PT powder after mechanochemical activation for (b) 30 h, (c) 70 h, and (d) 30 h and heating at 400 °C.

functional nanocrystalline materials[29] that has extensively been applied to the synthesis of ferroelectric powders[30−33] and to the processing of piezoelectric ceramics from them.[31−34] The technique allows most known perovskites to be mechanosynthesized,[31−33] which includes PMN,[35] PZN,[36] and their solid solutions with PT,[37,38] and high-quality PMN−PT ceramics with very good electrostrictive and piezoelectric properties have been processed.[37,39]

Experimental Section

Mechanochemical Activation Experiments. Experiments on three different perovskite solid solutions with a morphotropic phase boundary are reported here. These are $Pb(Zn_{1/3}Nb_{2/3})O_3-PbTiO_3$ (PZN−PT), $Pb(Zn_{1/3}Nb_{2/3})O_3-Pb(Fe_{1/2}Nb_{1/2})O_3-PbTiO_3$ (PZN−PFN−PT), and $BiScO_3-PbTiO_3$ (BS−PT). Compositions around their MPBs were investigated. Analytical grade PbO (Merck, 99%), ZnO (Sigma-Aldrich, 99.99%), Nb_2O_5 (Sigma-Aldrich, 99.9%), TiO_2 (anatase, Cerac, 99.9%), Fe_2O_3 (Cerac, 99.9%), Bi_2O_3 (Aldrich, 99.9%), and Sc_2O_3 (Aldrich, 99.9%) were used as precursors. In all cases, 3−4 g of a stoichiometric mixture was initially homogenized by hand in an agate mortar and placed in a

(29) Giri, A. K. *Adv. Mater.* **1997**, *9*, 163.
(30) Ferrer, P.; Iglesias, J. E.; Castro, A. *Chem. Mater.* **2004**, *16*, 1323.
(31) Lee, S. E.; Xue, J. M.; Wan, D. M.; Wang, J. *Acta Mater.* **1999**, *47*, 2633.
(32) Hungría, T.; Algueró, M.; Hungría, A. B.; Castro, A. *Chem. Mater.* **2005**, *17*, 6205.
(33) Hungría, T.; Algueró, M.; Castro, A. *Chem. Mater.* **2006**, *18*, 5370.
(34) Moure, A.; Castro, A.; Pardo, L. *Acta Mater.* **2004**, *52*, 945.
(35) Wang, J.; Junmin, X.; Dongmei, W.; Weibeng, Ng. *J. Am. Ceram. Soc.* **1999**, *82*, 1358.
(36) Wang, J.; Dongmei, W.; Junmin, X.; WeiBeng, Ng. *J. Am. Ceram. Soc.* **1999**, *82*, 477.
(37) Wang, J.; Wan, D. M.; Kue, J. M.; Ng, W. M. *Adv. Mater.* **1999**, *11*, 210.
(38) Algueró, M.; Ricote, J.; Castro, A. *J. Am. Ceram. Soc.* **2004**, *87*, 772.
(39) Algueró, M.; Moure, A.; Pardo, L.; Holc, J.; Kosec, M. *Acta Mater.* **2006**, *54*, 501.

stainless-steel pot with five 2 cm diameter, 35 g mass, also stainless-steel balls. Mechanochemical activation was carried out with a Pulverizette 6 model Fritsch planetary mill operating at 300 rpm.

Phases after mechanical activation of the powders and after thermal treatments were monitored by Bragg−Brentano X-ray diffraction (XRD) with a Bruker AXS D8 Advance diffractometer. Cu Kα radiation ($\lambda = 1.5418$ Å) and a 6.6×10^{-2} deg s^{-1} scan rate were used. Powder morphology and chemical homogeneity were studied by transmission electron microscopy (TEM). Dispersed particles were observed with either a Philips Tecnai-20 FEG apparatus working at 200 kV or a Philips CM20 microscope working at 200 kV, both equipped with an energy-dispersive X-ray spectrometer.

Ceramic Processing and Characterization. About 1 g of powder was uniaxially pressed into 12 mm pellets and further consolidated by isostatic pressure at 200 MPa. Sintering was carried out in a closed Al_2O_3 crucible in a conventional furnace. A temperature of 1100 °C, a holding time of 1 h, and heating/cooling rates of ±3 °C min^{-1} were used. A PbO-rich atmosphere was created in the case of PZN−PFN−PT by burying the pellets in $PbZrO_3$ powder.

Phases in the ceramics were determined by X-ray diffraction with a Siemens D500 powder diffractometer with Cu Kα radiation and a scan rate of 1×10^{-2} deg s^{-1}. Density was evaluated by the Archimedes method. Samples for microstructural characterization were prepared by polishing, thermal etching, and quenching. An optical microscope (Leitz Laborlux 12 ME ST) and a scanning electron microscope (SEM 960 Zeiss, 10−20 kV operation voltage, C-coated samples) equipped with an energy-dispersive X-ray spectrometer were used.

Ag electrodes were painted on the major faces of thinned disks and sintered at 650 °C for electrical characterization and poling. The temperature dependence of the dielectric permittivity was measured with an HP 4284A precision LCR meter at frequencies between 1 and 500 kHz as a means of determining the Curie temperature. d_{33} piezoelectric coefficients after poling were measured with a Berlincourt-type meter.

Results and Discussion

$Pb(Zn_{1/3}Nb_{2/3})O_3-PbTiO_3$. The process of mechanosynthesis of $0.92Pb(Zn_{1/3}Nb_{2/3})O_3-0.08PbTiO_3$ and its thermal decomposition has already been described;[38] ZnO, Nb_2O_5, and TiO_2 precursors are readily amorphized during the first hour of mechanical activation in air, along with severe particle size reduction of PbO. Nanometer-scale chemical homogeneity is obtained before 20 h, yet PbO nanoparticles are still present at this time. The perovskite is the only crystalline phase after activation for 30 h, and full crystallization is achieved at 70 h. The XRD pattern of the perovskite nanocrystalline powder obtained after mechanochemical activation for 70 h is shown in Figure 1a. However, the phase is not stable under heating above 400 °C, and a pyrochlore phase results. This is illustrated in Figure 1b, where the pattern of the perovskite powder of Figure 1a after heating at 700 °C is shown. The mass was carefully controlled during the thermal treatment, and losses were found to be negligible.

New experiments concentrated on the mechanochemical activation of the pyrochlore powder obtained by heating of the nanocrystalline perovskite. A relevant main result was the observation that the perovskite can be recovered by mechanochemical activation of the pyrochlore phase. This is shown in Figure 1c−g. Also, the activation time required for the perovskite to be the only crystalline phase by XRD, 16 h, is reduced as compared with the case of the mechanochemical activation of the oxides, 30 h.[38] This phenomenology is analogous to that found in high-pressure experiments,[23] for which the pressure required to obtain the perovskite was lower when the pyrochlore phase, a product of the solid-state reaction of the oxides, was used instead of the oxides, the activation playing the role of the pressure in mechanochemical activation.

$Pb(Zn_{1/3}Nb_{2/3})O_3-Pb(Fe_{1/2}Nb_{1/2})O_3-PbTiO_3$. The thermodynamic instability of the nanocrystalline $0.92Pb(Zn_{1/3}Nb_{2/3})O_3-0.08PbTiO_3$ perovskite by mechanosynthesis prevented single-phase ceramics from being processed from these powders.[38] A procedure that has successfully been applied to process PZN−PT-based ceramics is the partial substitution of a high-tolerance-factor perovskite, such as $BaTiO_3$[19] and PZT[40] for PZN. We have investigated the addition of $Pb(Fe_{1/2}Nb_{1/2})O_3$ (PFN) as a means of stabilizing the perovskite phase. This is a magnetoelectric, multiferroic perovskite[41] with a slightly higher tolerance factor than PZN ($t = 1.00$) but smaller electronegativity difference. Also, an MPB has been described in the PFN−PT binary system at a composition very close to that of PZN−PT.[42] Two PFN substitutions for PZN were tested: 0.1PFN and 0.4PFN. They were chosen after a previous report of the processing of PZN−PFN ceramics by conventional means that showed only the pyrochlore phase for 0.9PZN−0.1PFN and the major perovskite phase for 0.6PZN−0.4PFN.[43] The main features of the mechanochemical activation and ceramic processing experiments are summarized here. Mechanosynthesis was achieved for all compositions investigated that covered the range $(0.9 - x)$PZN−0.1PFN−xPT with $0.08 \leq x \leq 0.12$ and $(0.6 - x)$PZN−0.4PFN−xPT with $x = 0.08$ and 0.09. This is illustrated in Figure 2 for 0.82PZN−0.1PFN−0.08PT, where XRD patterns of the initial oxides and of the powder after increasing activation times are shown. The addition of Fe_2O_3 in the system does not modify the process of mechanosynthesis as already described for PZN−PT. The morphology of the perovskite powder is illustrated in Figure 3a. The powder consists of submicrometer size particles as shown by the TEM image. Selected area electron diffraction (SAED) indicates that these particles are tight aggregates of perovskite nanocrystals. SAED patterns of the particles after activation for 30 and 70 h are shown in Figure 3b,c. Well-defined rings with associated planar distances corresponding to those of the perovskite were found, in good agreement with XRD. Residual oxides or the amorphous phase were not observed, which indicates that the mechanosynthesis is completed after activation for 30 h. Energy-dispersive X-ray spectroscopy (EDXS) indicated the chemical homogeneity of the powder and the presence of an excess of Fe after the activation for 70 h, which was not observed in the powder mechanochemically activated for 30 h.

(40) Fan, H.; Kim, H. E. *J. Appl. Phys.* **2002**, *91*, 317.
(41) Fiebig, M. *J. Phys. D: Appl. Phys.* **2005**, *38*, R125.
(42) Suchomel, M. R.; Davis, P. K. *J. Appl. Phys.* **2004**, *96*, 4405.
(43) Yokosuka, M. *Jpn. J. Appl. Phys.* **1999**, *38*, 5488.

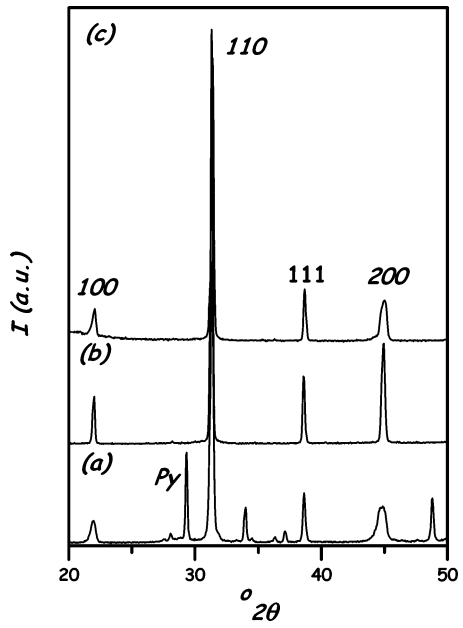

Figure 4. XRD patterns of 0.82PZN−0.1PFN−0.08PT ceramics processed from the nanocrystalline perovskite powder obtained by mechanochemical activation for (a) 30 h and (b) 70 h. (c) Pattern of a 0.52PZN−0.4PFN−0.08PT ceramic from the powder by mechanosynthesis. Perovskite peaks are labeled with the Miller indices assigned on the basis of a pseudocubic unit cell. Py = pyrochlore.

The perovskite was still not stable under heating at temperatures above 400 °C, and a pyrochlore phase resulted, yet the amount of remnant perovskite phase after a given temperature profile clearly increased with the addition of PFN. This allowed the processing of perovskite ceramics virtually free of the pyrochlore phase by sintering at 1100 °C. XRD patterns for PZN−PFN−PT dense ceramics processed from the powders by mechanosynthesis are shown in Figure 4. Ceramics of composition (0.9 − *x*)PZN−0.1PFN−*x*PT processed from powders mechanochemically activated for 30 h showed a minor amount of pyrochlore phase that disappeared when powders activated for 70 h were used (Figure 4a,b). Note that the 200 diffraction peak of the perovskite for the 0.82PZN−0.1PFN−0.08PT ceramics is much broader for the ceramic from 30 h powders than for the ceramic from 70 h powders. This indicates that the perovskite composition is at the morphotropic phase boundary for the ceramic from the powder activated for 30 h and that this composition shifts toward the rhombohedral end, i.e., toward the PZN/PFN, with further activation. Perovskite-phase ceramics free of pyrochlore were obtained for (0.6 − *x*)PZN−0.4PFN−*x*PT (Figure 4c). Densifications above 95% were achieved for both compositions. The microstructure of the 0.82PZN−0.1PFN−0.08PT ceramic from the powder activated for 30 h, which presented some minor pyrochlore phase according to XRD (Figure 4a), is shown in Figure 5. Coarse grains (∼5 μm), labeled A, appear together with fine grains (<1 μm), labeled B, and some isolated grains, which show a different contrast, labeled C. This different contrast of grains C is due to their different composition, which can be ZnO according to the EDXS results carried out in the scanning electron microscope. This microanalysis also showed that grains B are Pb and Zn deficient in relation to grains A. According to the XRD results, grains A are most probably the perovskite phase while grains B are the pyrochlore phase. These results support that the process by which the pyrochlore is obtained from the mechanosynthesized perovskite by heating is a chemical decomposition into pyrochlore, ZnO, and PbO. The possibility that ZnO is

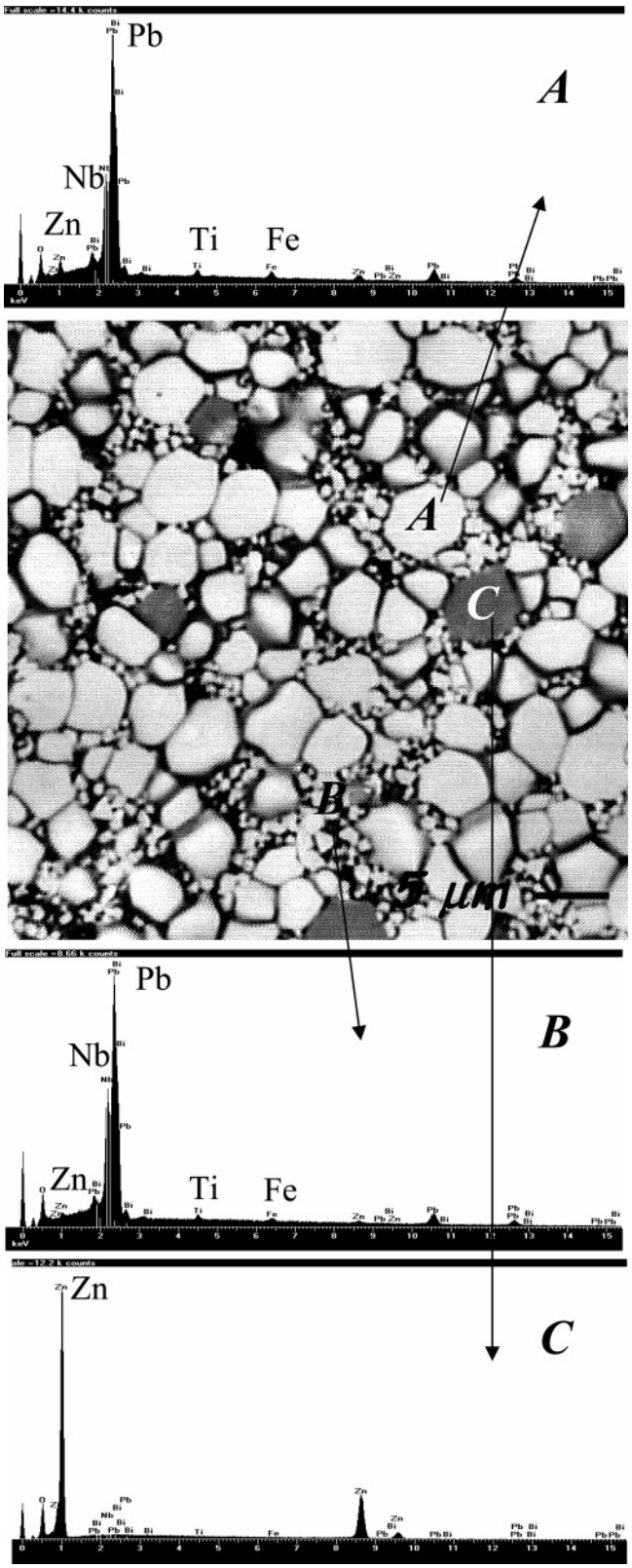

Figure 5. Microstructure of an 0.82PZN−0.1PFN−0.08PT ceramic processed from the nanocrystalline perovskite powder obtained by mechanochemical activation for 30 h. Labels A−C correspond to the three microstructural features on which EDXS was carried out.

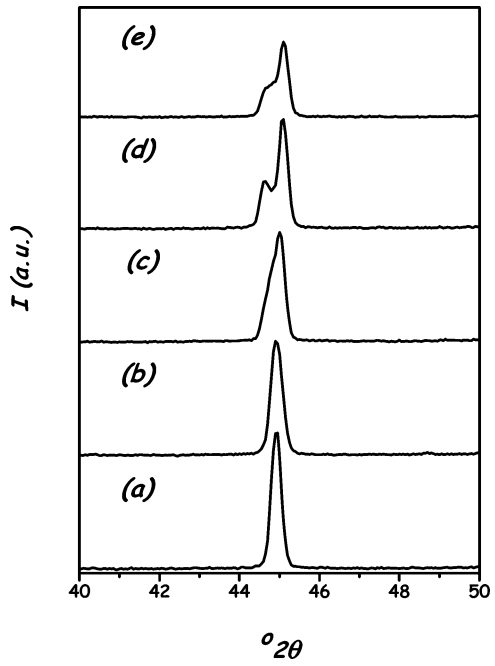

Figure 6. XRD 200 peak for $(0.9 - x)$PZN−0.1PFN−xPT ceramics with (a) $x = 0.08$, (b) $x = 0.09$, (c) $x = 0.10$, and (d) $x = 0.12$. (e) XRD 200 peak for a 0.52PZN−0.4PFN−0.08PT ceramic.

already present in the powder was ruled out by studying a sample of the mechanosynthesized 0.82PZN−0.1PFN−0.08PT powder heated at 400 °C, which is below the temperature at which the pyrochlore phase appears, by transmission electron microscopy and EDXS. The morphology did not change after heating, and the powder still consisted of agglomerates of nanocrystals as shown by the SAED pattern of Figure 3d. Neither ZnO nanoparticles nor Zn-rich particles were found. Therefore, ZnO is a product of the decomposition of the perovskite phase and not the remains of the initial oxides.

All these results show that mechanosynthesis allows the processing of virtually pyrochlore free, perovskite-dense ceramics for compositions of the ternary PZN−PFN−PT system that cannot be processed by solid-state synthesis.[43] The highest piezoelectric coefficients are found for compositions near the MPBs, and the PZN−PFN−PT ternary system is no exception. We investigated the occurrence of an MPB by studying the evolution of the pseudocubic 200 diffraction peak when the PT content was increased. This is shown in Figure 6a−d for $(0.9 - x)$PZN−0.1PFN−xPT ceramics with x from 0.08 to 0.12. The evolution from a single peak (rhombohedral structure) to a double peak (tetragonal structure) is evident. The peak for a 0.52PZN−0.4PFN−0.08PT ceramic is shown in Figure 6e, suggesting its proximity to the MPB. A d_{33} piezoelectric coefficient of 220 pC N^{-1} was obtained after poling at 50 °C and 3.0 kV mm^{-1} for the latter ceramic, which is comparable to the values of undoped MPB PZT materials. This demonstrates the feasibility of processing high-sensitivity piezoelectric, low-tolerance-factor PZN−PT-based ceramics by mechanosynthesis.

$BiScO_3$−$PbTiO_3$. The generality of the approach, i.e., that mechanosynthesis allows the processing of ceramics of not only PZN−PT-based compositions but also other high-sensitivity piezoelectric, low-tolerance-factor perovskites that cannot be obtained by solid-state reactions, is demonstrated with the $BiScO_3$−$PbTiO_3$ (BS−PT) system. Mechanosynthesis was achieved for $(1 - x)$BS−xPT compositions with $0.4 \leq x \leq 0.64$, as illustrated for $x = 0.4$ in Figure 7. Like PZN−PFN−PT powders, the BS−PT powders consisted of submicrometer size, tight aggregates of nanocrystals. SAED patterns of the 0.6BS−0.4PT powder after activation for 70 and 140 h are also shown in the figure. Nanocrystalline phases other than perovskite, residual oxides and intermediate phases, and the amorphous phase are observed for the powder activated for 70 h, but not for that activated for 140 h, in agreement with XRD. These studies showed that the mechanical activation time required to complete the mechanosynthesis decreased as x increased across the $(1 - x)$BS−xPT solid solution, so 70 and 35 h were enough for obtaining a single nanocrystalline perovskite with $x = 0.5$ and 0.6, respectively. EDXS indicated chemical homogeneity beginning at 35 h, the time after which Fe contamination was not significant. Fe was found in the powder activated for 70 h (∼2 atom %), and its amount increased with further activation (∼4 atom %).

XRD patterns for ceramics processed from the mechanosynthesized powders are shown in Figure 8. Patterns a and b correspond to 0.6BS−0.4PT ceramics prepared from perovskite powders obtained by mechanochemical activation for 70 and 140 h, respectively. Note the presence of some secondary phase for the material processed from powder activated for 70 h that disappears for that processed from the powder activated for 140 h. This $BiScO_3$-rich composition ($t = 0.95$) cannot be synthesized by solid-state reaction of the oxides, but has only been obtained by high-pressure synthesis.[28] This result confirms that there is an apparent equivalence between mechanochemical activation in planetary mills and the application of high pressures and temperatures, the activation time playing a role similar to the pressure.

The processing of BS−PT ceramics with different compositions across the MPB from those of the mechanosynthesized powders has also been accomplished. XRD patterns c and d in Figure 8 correspond to ceramics of 0.5BS−0.5PT, from a powder activated for 70 h, and 0.35BS−0.65PT, from a powder activated for 35 h, which show the evolution from the rhombohedral to the tetragonal structure. It must be noted that 0.5BS−0.5PT obtained by high-pressure synthesis has been reported to be pseudocubic instead of rhombohedral, and a relaxor state was proposed to exist.[28] However, the authors also reported a maximum of remnant polarization of 56 μC cm^{-2} for this composition, which is not consistent with such a polar state, but suggests that a ferroelectric phase is present. The discrepancy is most probably due thus to differences in the size of the rhombohedral domains between the samples obtained by high-pressure synthesis and mechanosynthesis.

Stabilization Mechanism and Associated Effects. Analogies between high-temperature high-pressure techniques and mechanochemical activation in high-energy planetary mills have to be raised with care, for the stress states involved are different; a constant hydrostatic-like pressure is applied in the former case, while intermittent compressive and shear

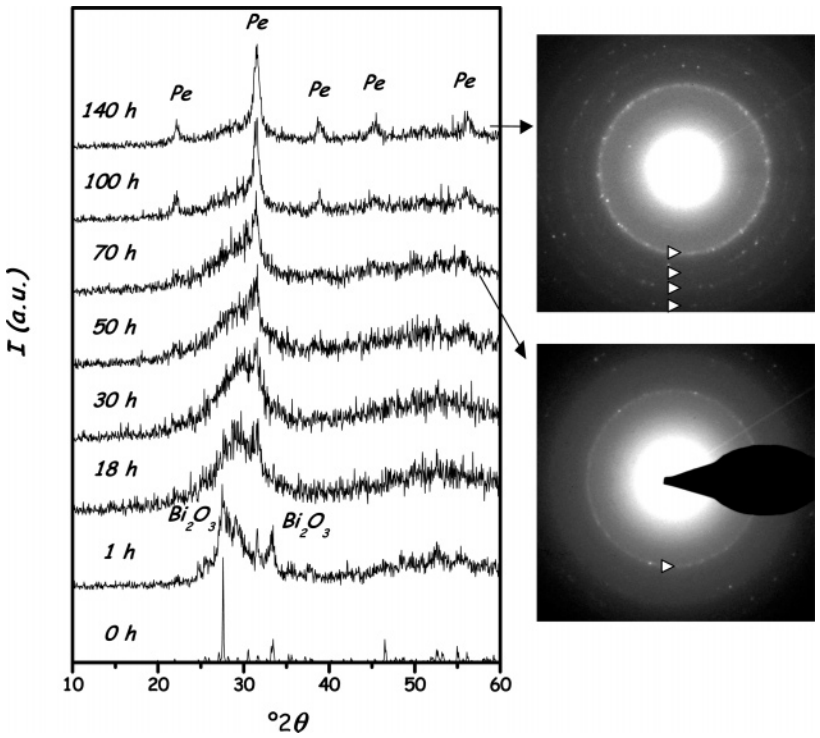

Figure 7. XRD patterns of the 0.6BS−0.4PT precursor powder after mechanochemical activation at increasing times. Pe = perovskite. SAED patterns for the powder after activation for 70 and 140 h are shown.

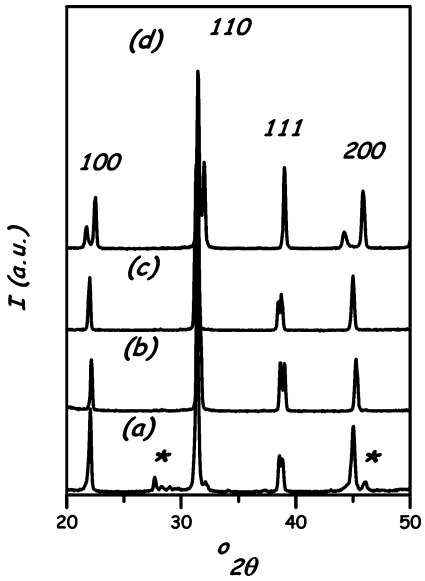

Figure 8. XRD patterns for 0.6BS−0.4PT ceramics processed from the nanocrystalline perovskite powder obtained by mechanochemical activation for (a) 70 h and (b) 140 h. Patterns of (c) 0.5BS−0.5PT and (d) 0.35BS−0.65PT ceramics from the powder by mechanosynthesis. Perovskite peaks are labeled with the Miller indices. The asterisks indicate the secondary phase.

stresses are generated during the collisions within the mill. Nevertheless, we have experimentally observed similar effects of pressure and mechanical activation time on perovskite stabilization in the two types of experiments, and both allow low-tolerance-factor perovskites to be synthesized.

The stabilization mechanism under high pressure is the high compressive hydrostatic-like strain imposed on the material. This is maintained on cooling and relaxed at low temperature, at which the material becomes stabilized. Nanocrystalline phases obtained by mechanochemical activation are known to present a high level of disorder and defects that result in a high average crystalline strain. This strain can be decomposed into different components, one of the hydrostatic type that would be thus responsible for the stabilization as already proposed by Shinohara et al., who studied the synthesis of $Pb(Zn_{1/3}Nb_{2/3})O_3-Pb(Mg_{1/3}Nb_{2/3})O_3$ by a soft mechanochemical route.[44] The crystalline strain is accumulative with the mechanochemical activation time, which explains the apparent equivalence between pressure and activation time in the two techniques.

The feasibility of processing ceramics from the highly crystal strained perovskite powder by mechanosynthesis rests on the relative kinetics of strain relaxation and sintering, that is, densification and grain growth, during heating. The FWHM of the XRD peaks of ceramics processed at 1100 °C increases with the mechanochemical activation time of the powders; for instance, it is $2\theta = 0.1877°$ for the 111 peak of tetragonal 0.35BS−0.65PT from the powder activated for 35 h and $2\theta = 0.1977°$ for a material from the powder activated for 70 h. This indicates that an increasing level of crystalline strain is retained in the ceramics after sintering. Also, the unit cell volume of the perovskite decreases when the mechanical activation time increases, from 64.76 to 64.18 Å^3 for ceramics from the powder activated for 35 and 70 h, respectively. This is consistent with the existence of a compressive hydrostatic-like component in the average crystalline strain.

An issue that is immediately raised is how this crystalline strain affects the properties of the materials. This has to be addressed in a system for which materials had been processed by solid-state reactions and were well characterized, and the BS−PT is an obvious choice.[24,27] A first effect is the slight

(44) Shinohara, S.; Baek, J. G.; Isobe, T.; Senna, M. *J. Am. Ceram. Soc.* **2000**, *83*, 3208.

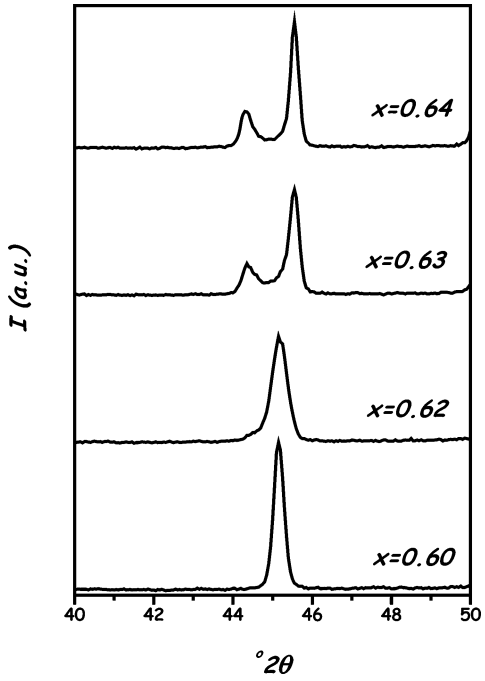

Figure 9. XRD 200 peak for $(1 - x)$BS$-x$PT ceramics processed from the nanocrystalline perovskite powder obtained by mechanochemical activation for 35 h.

shift of the composition of the MPB toward the BS edge in the crystal-strained material as compared to that synthesized by solid-state reaction. This is illustrated in Figure 9, where the pseudocubic 200 diffraction peak of $(1 - x)$BS$-x$PT ceramics with x between 0.6 and 0.64 processed from the powder activated for 35 h is shown. Note that the MPB is at $x \approx 0.62$, while it is at 0.64 for the materials by solid-state reactions reported in the literature.[24,27,28]

This shift is confirmed by the variation of the piezoelectric coefficient with composition for the crystal-strained material. This is shown in Figure 10a along with previous results by Eitel et al. on ceramics from powders by solid-state reactions.[24,27] All materials were poled at 4 kV mm^{-1} at 100 °C. Maximum d_{33} coefficients were obtained at $x = 0.62$ and 0.64 for the ceramics by mechanosynthesis and solid-state reactions, respectively, in good agreement with the positions of the MPB by XRD. The piezoelectric coefficient for the crystal-strained MPB BS−PT was 330 pC N^{-1}. This is lower than that of the crystalline strain-free material, but still higher than that of MPB PZT.

The Curie temperature, T_C, as a function of composition across the crystal-strained BS−PT is shown in Figure 10b, also compared with previous results on ceramics from powders by solid-state reactions. These values correspond to the maxima in the temperature dependence of the permittivity associated with the ferroelectric to paraelectric phase transition, which is shown in the inset for a 0.38BS−0.62PT ceramic as an example. Note that T_C figures are slightly lower for the crystal-strained material than for the ceramics processed by solid-state reactions. The Curie temperature for the crystal-strained MPB material was 425 °C, which is lower than that of the crystalline strain-free material, but still significantly higher than that of MPB PZT, 385 °C. Note also that a similar slope with composition is obtained for the two cases. This is a strong indication that

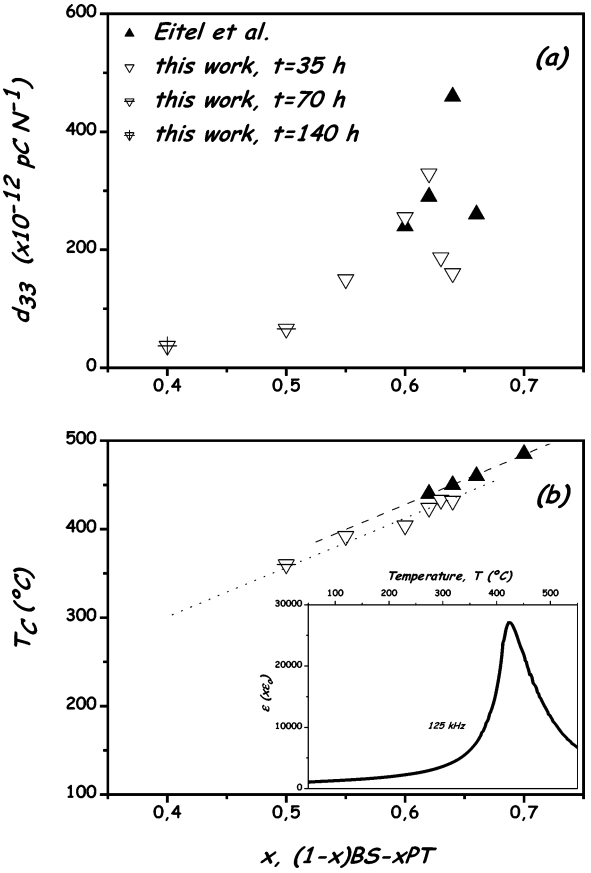

Figure 10. (a) d_{33} piezoelectric coefficient and (b) Curie temperature, T_C, for $(1 - x)$BS$-x$PT ceramics processed from powders obtained by solid-state reactions (after Eitel et al.[24,27]) and by mechanosynthesis (this work). An increasing mechanochemical activation time, t, was necessary for processing the ceramics as x was decreased as indicated in the legend. The inset in (b) shows the temperature dependence of the dielectric permittivity for a 0.62BS−0.38PT ceramic by mechanosynthesis.

perovskite composition deviations do not exist in the ceramics by mechanosynthesis and that the solid solution is formed in the composition range investigated.

Figure 10 includes the properties of 0.5BS−0.5PT and 0.6BS−0.4PT ceramics that cannot be obtained by conventional means, which are consistent with the observed trends with composition for $x \geq 0.55$. Note that T_C for $x = 0.4$ is not given because the maximum of permittivity associated with the transition is overlapped with a high-temperature Debye-type relaxation, most probably associated with the large concentration of defects present in this ceramic processed from powder mechanochemically activated for 140 h.

An additional issue that needs to be discussed is contamination from the milling media, Fe in this case, which has been observed by EDXS in the powders activated for times longer than 35 h. Its presence during the mechanosynthesis of BS−PT can result in the formation of $BiFeO_3$, also a multiferroic perovskite like $Pb(Fe_{1/2}Nb_{1/2})O_3$,[41] with a tolerance factor ($t = 0.947$) higher than that of $BiScO_3$ ($t = 0.903$). Therefore, its incorporation in the solid solution to form the ternary system $(1 - y)$BS$-y$BF−PT would improve the perovskite stability. Though this mechanism most probably adds up to that of the crystalline strain to stabilize the perovskite, it is not the dominant mechanism because associated effects are not consistent with it; the Curie

temperature of $BiFeO_3$ is 836 °C,[45] and a significant increase in T_C should result from the formation of the ternary system, which was not observed (see T_C for the ceramic with $x = 0.5$, which was processed from powder mechanochemically activated for 70 h).

In summary, crystalline strain generated during the mechanosynthesis is most probably the mechanism responsible for the stabilization of the low-tolerance-factor perovskites. This crystal strain slightly shifts the position of the MPB toward the rhombohedral edge of the BS−PT solid solution and decreases the piezoelectric coefficient and Curie temperature of the material. Nevertheless, the crystal-strained MPB BS−PT material is still a high-sensitivity, high-Curie-temperature material with properties better than those of MPB PZT.

Summary and Conclusions

It has been shown that the activation time required for the mechanosynthesis of $0.92Pb(Zn_{1/3}Nb_{2/3})O_3-0.08PbTiO_3$ in a planetary mill is reduced when a stoichiometric mixture of pyrochlore phase, ZnO, and PbO is used instead of the binary oxides, an effect analogous to the reduction of the pressure required for the high-pressure synthesis. Mechanosynthesis is also achieved for compositions in the systems $Pb(Zn_{1/3}Nb_{2/3})O_3-Pb(Fe_{1/2}Nb_{1/2})O_3-PbTiO_3$ and $BiScO_3-PbTiO_3$ that had not been obtained before, but at very high pressures. Mechanosynthesis is thus a good alternative to high-pressure synthesis for the preparation of low-tolerance-factor perovskites. It provides enough material for addressing complete processing studies and the full assessment of material functionality. It has a huge potential in the search for novel MPB systems for the development of new high-sensitivity piezoelectric materials. This has been demonstrated by processing ceramic materials of MPB $Pb(Zn_{1/3}Nb_{2/3})O_3-Pb(Fe_{1/2}Nb_{1/2})O_3-PbTiO_3$ and $BiScO_3-PbTiO_3$. The problems related to the perovskite stability, which can be addressed with mechanochemical activation as shown here, are not limited to piezoelectrics, but it is relevant to other material technologies, such as colossal magnetoresistance,[46] or magnetoelectric materials.[41]

Acknowledgment. This research has been funded by MEC (Spain) with the MAT2004-00868 and MAT2005-01304 projects. Part of the transmission electron microscopy studies were carried out at the facilities of the Universidad Carlos III de Madrid (Spain).

CM071656V

(45) Woodward, D. I.; Reaney, I. M.; Eitel, R. E.; Randall, C. A. *J. Appl. Phys.* **2003**, *94*, 3313.

(46) Haghiri-Gosnet, A. M.; Renard, J. P. *J. Phys. D: Appl. Phys.* **2003**, *36*, R127.